International Journal of Biological Macromolecules 242 (2023) 124941

Contents lists available at ScienceDirect

International Journal of Biological Macromolecules

journal homepage: www.elsevier.com/locate/ijbiomac

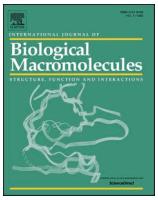

Oleogels and reverse emulsions stabilized by acetylated Kraft lignins

Antonio M. Borrero-López [a,*], Ling Wang [b], Haiming Li [b,c], Tainise V. Lourençon [b], Concepción Valencia [a], José M. Franco [a], Orlando J. Rojas [b,d,e]

[a] Pro2TecS – Chemical Process and Product Technology Research Centre, Dept. Ingeniería Química, ETSI, Campus de "El Carmen", Universidad de Huelva, 21071 Huelva, Spain
[b] Department of Bioproducts and Biosystems, School of Chemical Engineering, Aalto University, P.O. Box 16300, FIN-00076 Espoo, Finland
[c] Liaoning Key Lab of Lignocellulose Chemistry and BioMaterials, Liaoning Collaborative Innovation Center for Lignocellulosic Biorefinery, College of Light Industry and Chemical Engineering, Dalian Polytechnic University, Dalian 116034, China
[d] Department of Applied Physics, School of Science, Aalto University, P.O. Box 16300, FIN-02150 Espoo, Finland
[e] Departments of Chemical and Biological Engineering, Chemistry and Wood Science, 2360 East Mall, The University of British Columbia, Vancouver, BC V6T 1Z3, Canada

ARTICLE INFO

Keywords:
Oil structuring
Lignin nanoparticles
Microwave-assisted acetylation
Pickering emulsions
Rheology

ABSTRACT

Acetylated Kraft lignins were evaluated for their ability of structuring vegetable oils into oleogels. Microwave-assisted acetylation was used to adjust lignin's degree of substitution according to reaction temperature (130 to 160 °C), and its effect in improving the viscoelasticity of the oleogels, which was related to the hydroxyl group content. The results were compared with those obtained by Kraft lignins acetylated using conventional methods at room temperature. A higher microwave temperature resulted in gel-like oil dispersions with improved viscoelastic properties, and stronger shear-thinning character, along with enhanced long-term stability. Lignin nanoparticles structured castor oil by enhancing hydrogen bonding between the hydroxyl groups of the oil and the nanoparticles. The oil structuring capacity of the modified lignins enhanced the stability of water-in-oil Pickering emulsions that resulted from low-energy mixing.

1. Introduction

The materials that structure oils are highly appreciated in the food, cosmetics and lubricant sectors. Ideally, renewable structuring agents should reduce or substitute those in current use, which usually raise health and environmental concerns [1,2]. Crystalline triacylglycerols, generally highly concentrated in trans- and/or cis-saturated fats, have been traditionally used for oil structuring [3]. Nonetheless, they are associated with obesity issues [4], posing a potential risk to human health. On the other hand, metallic-based soaps have been adopted as gelling agents in the synthesis of lubricating greases [5,6]. Together with the use of petroleum-derived mineral oils [7,8], their discharge in water streams poses a major threat to water quality and aquatic life [7,9]. As a consequence, inert and renewable gelling agents for oil media are highly desirable. Alternatives such as mono- and di-acylglycerols, natural waxes, sphingolipids and cellulose-based agents, as well as inorganic particles such as fumed silica, have been reported related to the food industry [3].

Likewise, to improve the performance and provide greener alternatives to common lubricating greases, biosourced thickening agents such as cellulose [10–12], chitosan [13,14] or lignin [2,15–18] have been considered. However, some incompatibilities may raise given their different polarities relative to that of the oil. Indeed, compared to standard lubricating greases, bio-based oleogels generally demand higher thickener concentrations to preserve mechanical and physical stability resulting in much higher viscoelastic moduli [19]. To overcome these drawbacks, crosslinking through diverse isocyanate and epoxy compounds has been applied [2,15,16,20,21], eventually approaching the performance of commercial lubricating greases [10,19,21]. Additionally, environmentally benign treatments have been applied for oil structuring [2,22]. Many pretreatments are biological, through the action of fungi or bacteria [2], but also nanotechnologies have been applied to enhance oil structuring [23,24]. An alternative pathway consists of biosource hydrophobization, for example, by replacing hydroxyl groups with other non-polar functional moieties such as acyls [14,25].

Of significance to this work is the case of lignin, which is well positioned considering factors such as intrinsic properties and upcoming

* Corresponding author.
E-mail address: am.borrero@diq.uhu.es (A.M. Borrero-López).

https://doi.org/10.1016/j.ijbiomac.2023.124941
Received 31 March 2023; Received in revised form 3 May 2023; Accepted 15 May 2023
Available online 19 May 2023

demand-pull. The potential of lignin is also highlighted by its availability, given that only 2 % of the lignin produced in the pulp and paper industry is directed to value-added materials, with the balance used in energy and chemical co-generation [9,26]. Structurally, lignin comprises methoxylated phenyl-propane units and functional groups linked with a wide range of bond types [27,28]. For oil structuring purposes, lignin modification may also be required to improve compatibility and/or reactivity, as recently demonstrated [2,15]. Other uses, such as oil-in-water Pickering emulsion stabilization are well documented [29–32]; however, the opposite cannot be said of lignin-based water-in-oil emulsions [33,34]. This latter type of emulsions represents a platform for oil structuring, which is associated with spreadability and moisturizing effects in food, cosmetics, delivery vehicles and other formulations [35,36].

This study investigates modified Kraft lignin nanoparticles as structuring components of castor oil that provide gel-like viscoelastic characteristics and significantly increase its viscosity, especially in emulsified forms. A main consideration relates to the lignin particle source, obtained as-is (by mechanical shearing) or following acetylation (by conventional and microwave-assisted methods). We unveil the thickening and stabilizing effects of particulate lignin forms in vegetable oil, especially relevant for the substitution of environmentally harmful thickeners or crosslinkers.

2. Materials & methods

2.1. Materials

Indulin AT, a softwood Kraft lignin (1.3 wt% sulfur content) [37] with a median particle size of 363 μm [38] was purchased from Mead-Westvaco (USA) and thereafter referred to as KL. Castor oil (CO) (purity not indicated), acetic anhydride (purity >99 %), Nile Red (purity ≥97 %), and solvents (pyridine (purity ≥99 %), deuterated chloroform (purity ≥99.8 %), HCl (37 wt%) solution) were obtained from Merck-Sigma Aldrich (Finland) and used as received. Lignin nanoparticles (NP) from Indulin AT were obtained by the dry method (aerosolization, as introduced in our earlier work) [39].

2.2. Acetylation

Conventional lignin acetylation was carried out by using 2 g of lignin and 48 mL of 1:1 (v/v) pyridine:acetic anhydride mixture in a round-bottom vessel and stirred at room temperature for 48 h. Thereafter, 10-fold volume of 1 wt% HCl solution at 0 °C was poured into the vessel in order to precipitate the acetylated Kraft lignin (from now on, referred to simply as acetylated lignin). Then, the acetylated lignin was washed and filtered several times with distilled water until no residual reactants were present. Finally, drying was carried out in a convection oven at 40 °C for at least two days to completely eliminate water [2,40]. The acetylated lignin obtained by this method was labeled as FAcKL.

The microwave-assisted acetylation was accomplished by using a Monowave 300 microwave synthesis reactor from Anton Paar (Austria). In a typical experiment, no solvent or catalysts were added. Lignin (2 g) and acetic anhydride (10 mL) were placed in a 30 cm^3 glass vessel and the mixture was then mechanically stirred at a given temperature (from 130 to 160 °C) and irradiated at ~850 W for 10 min. Washing and drying were performed as indicated above for the reference method used to obtain acetylated lignins. The obtained acetylated lignin samples were labeled as "AcKL" and named using the processing temperature in °C, namely, AcKL-130, AcKL-140, AcKL-150 and AcKL-160. The two lignin types and NPs are generically referred to as Modified Lignins (ML).

2.3. Imaging

Optical microscopy images at different magnifications were obtained using a Leica DM4500 P microscope (Germany). For confocal microscopy, a Leica DMRXE microscope (Germany) equipped with an HC PL APO 20×/0.70 CS objective was used. Prior to observation, fluorescence was accomplished by dying CO with Nile red (250 μL of 1 mg/mL Nile red/ethanol solution per 5 g of CO). SEM micrographs were taken using Zeiss Sigma VP equipment (Germany). Before imaging, samples were sputter-coated with iridium of 6 nm thickness by using a Leica EM ACE 600 High Vacuum Sputter Coater (Germany).

2.4. Thermal properties

The thermal stability of lignin, NPs and acetylated lignins (FAcKL and AcKL) was determined using a TGA Q500 (TA Instruments, USA) operating in N_2 atmosphere, from room temperature up to 600 °C (heating rate 10 °C/min). For each thermal event, the temperature at which degradation began (T_{onset}) and ended (T_{final}), the temperature corresponding to the maximum derivative weight loss (T_{max}) and weight loss percentage during the event are reported, as well as the final residue after the test (%).

2.5. Spectroscopic characterization

For FTIR characterization, a Nicolet 380 FT-IR (Thermo Scientific, USA) infrared spectrometer was used. Measurements were performed from 400 to 4000 cm^{-1} wavenumbers with a resolution of 4 cm^{-1}. The content of hydroxyl groups was determined by ^{31}P NMR [41,42] (Bruker NMR Spectrometer AV III 400, USA) in accordance with an optimized protocol previously developed [43]. Briefly, about 40 mg of each lignin was dissolved in 0.4 mL of pyridine and deuterated chloroform (1.6:1, v/v) solution. Then, 50 μL of chromium (III) acetylacetonate (11.4 mg in 1 mL of the solution) and a certain amount of internal standard (IS) (0.12 M *endo*-n-hydroxy-5-norbornene-2,3-dicarboximide), required to obtain an IS/lignin ratio of 1:20 *w*/w, were introduced. At the final stage, 100 μL of phosphorus-containing reagent (2-chloro-4,4,5,5-tetramethyl-1,3,2-dioxaphospholane) was added to the mixture. The vial content was vortexed, transferred into an NMR tube and tested in the NMR equipment. The acquisition time was 1 s, the relaxation delay was 5 s, and 128 scans were collected. The spectra were phased and calibrated using the signal of water-derivatized product (122.2 ppm). The baseline was corrected using a linear function. The degree of substitution of acetyl groups (DS) was calculated by considering the relative decrease in the total OH groups content in the AcKL or FAcKL compared to KL, by following the expression below:

$$DS\ (\%) = \left(1 - \frac{OH_{KL} - OH_{(F)AcKL}}{OH_{KL}}\right) \cdot 100 \quad (1)$$

^1H NMR spectra were acquired (Bruker NMR Spectrometer AV III 400, USA) using 20 mg of each lignin that were mixed with 0.6 mL of deuterated dimethyl sulfoxide (DMSO) containing 2 mg of IS pentafluorobenzaldehyde, keeping an IS/lignin ratio of 1:10 *w*/w. The acquisition time was 5.12 s, the relaxation delay was 25 s, and 128 scans were collected.

2.6. Water contact angle

The water contact angle (WCA) was measured by placing a 6-μL water droplet on the surface of disks of lignin and acetylated lignin, both prepared by mold pressing. For imaging, a Sigma 70 force tensiometer (UK), equipped with a COHU solid-state CCD monochrome camera was used. The results obtained were the average of the WCA of at least 5 water drops and, for each drop, the WCA value corresponds to an average value of the measurements taken every second during a 1 min test.

2.7. Preparation of colloidal dispersions

Gel-like dispersions were obtained by mechanical stirring of the modified lignins (MLs) (10 to 40 % *w*/w) and castor oil (CO) for 3 h. Other vegetable oils were also tested. The physical stability of the systems was assessed by visual observation of the oil phase separation. Phase separation percentage was quantified by digitally measuring the separated oil-phase height in relation to the total height of the sample, using a container of 24 mm diameter.

2.8. Rheology of colloidal dispersions

Small-amplitude oscillatory shear (SAOS) and viscous flow tests were performed in an Anton Paar Physica MCR302 rheometer (Austria) using a serrated plate-plate geometry (50 mm diameter, 1 mm gap). In SAOS measurements, the frequency range studied varied between 0.03 and 100 rad/s. The linear viscoelastic regime was previously determined by performing strain sweep tests. Viscous flow curves were obtained by applying an increased stepped shear rate ramp between 0.01 and 100 s^{-1} maintaining the shear rate for 3 min in each step. Experiments were replicated at least twice, unless the results differed too much from each other, when more replicates were analyzed.

2.9. Particle size of lignin in the dispersions

The size distribution of lignin particles in the gel-like dispersions was obtained by measuring the size of random particles in optical microscope images by using the image processing ImageJ 1.8.0_112/1.52a. Each size distribution was acquired from at least 500 measurements.

2.10. Preparation of W/O emulsions

For the preparation of the emulsions, water was added to ML/CO-based gel dispersions. The lignin concentration is used on a total emulsion weight basis (8–10 wt%). The blend was emulsified by using either a vortex stirrer or an IKA T25 Ultra-Turrax homogenizer at 10000 rpm. Emulsions with 10 wt% water and 90 wt% CO were produced and characterized (rheology, morphology), and up to 30 wt% water concentration was tested.

3. Results and discussion

3.1. Lignin and ML

Lignin acetylation was carried out by esterification of the hydroxyl groups as described above; accordingly, a decrease in -OH group content was observed (^{31}P NMR, Table 1 and Fig. S1). The lowest -OH content was determined for FAcKL, and a linear correlation between acetylation microwave-assisted temperature and the decrease of free -OH was observed (Fig. 1, hydroxyl groups content relative to acetyl groups per 100 aromatic units). The latter effect was concomitant with a gradual increase in esterification, which translates to a higher degree of substitution or acetylation, DS (Table 1). Consequently, this fact implies the possibility of tuning the acetylation degree by the temperature adjustment. The observed effect on free -OH was not replicated when phenolic or aliphatic acetyl groups were considered (^{1}H NMR). In fact, the differences in acetyl groups were much larger when changing the acetylation temperature from 130 to 140 °C, and thereafter the aliphatic acetyl group content remained relatively unchanged while the phenolic content exhibited a slight increase. These results relate to the high temperatures selected, which may produce some degree of degradation or side reactions. The highest acetyl group densities were obtained by following the conventional method.

The characteristic temperatures and weight losses associated with the main thermal events of KL and the MLs (Fig. 2) are shown in Table 2. The TGA spectra of the lignins (Fig. 2) exhibit main thermal degradation events related to the dehydration of the hydroxyl groups, centered at around 150–250 °C [44,45], and the breakage of the main inter-unit linkages of Kraft lignin [46], providing the main weight loss event at 340–380 °C [20,44,47]. It is worth noting that deacetylation is also possible, as reported to occur between 230 and 250 °C [40].

The dehydration of the hydroxyl groups (ca. 150–250 °C) provided small but significant weight losses, which can be related to the initial hydroxyl group content of each sample. The unmodified lignin (KL)

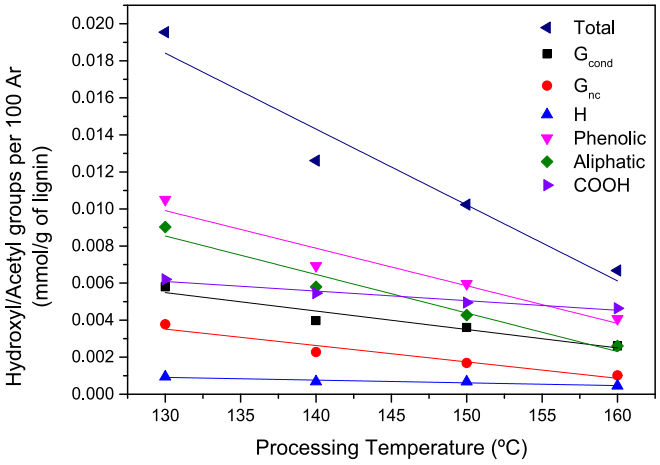

Fig. 1. Hydroxyl groups per number of acetyl groups in 100 aromatic units (diverse positions of the lignin chain, see Table 1) as a function of temperature used in the microwave-assisted acetylation (AcKL-130 to AcKL-160).

Table 1
^{31}P and ^{1}HNMR analysis of the neat unmodified lignin (KL) and the acetylated lignins (FAcKL, AcKL).

Sample	mmol/g of lignin							DS (%, ^{31}P NMR)	Phenolic acetyl groups (per 100 Ar units)	Aliphatic acetyl groups (per 100 Ar units)
	$G_{cond.}$	G_{nc}	H	Phenolic -OH	Aliphatic -OH	Total -OH	COOH			
KL	1.64	1.69	0.26	3.59	2.49	6.08	0.46	–	10.93	13.95
AcKL-130	0.43	0.28	0.07	0.78	0.67	1.45	0.46	76.15	30.54	43.70
AcKL-140	0.35	0.20	0.06	0.61	0.51	1.11	0.48	81.74	35.75	52.30
AcKL-150	0.32	0.15	0.06	0.53	0.38	0.91	0.44	85.03	36.40	52.49
AcKL-160	0.23	0.09	0.04	0.36	0.23	0.59	0.41	90.30	37.96	50.41
FAcKL	0.11	0.05	0.03	0.19	0.13	0.32	0.37	94.74	38.54	60.74

$G_{cond.}$: condensed guaiacyl, G_{nc}: non-condensed guaiacyl, H: *p*-hydroxyphenyl, Phenolic OH: $G_{cond.}$ + G_{nc} + H, Total OH: Phenolic OH + Aliphatic OH, COOH: carboxylic acid, Ar: aromatic.

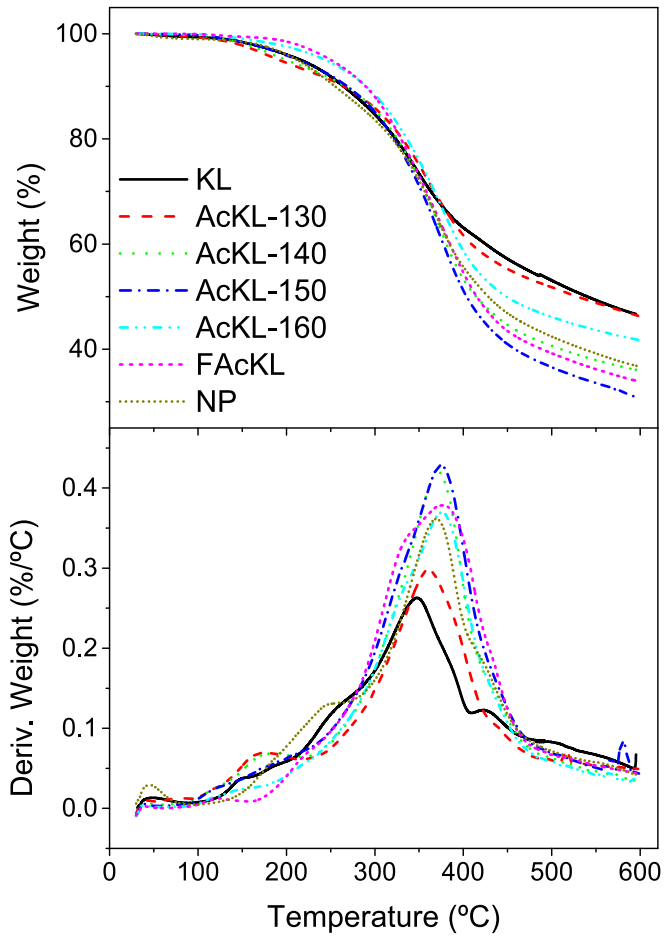

Fig. 2. Thermogravimetric curves, in the form of top) weight loss vs. temperature and bottom) its derivative for KL and ML samples.

Table 2
TGA characteristics parameters for KL and ML systems as well as lignin nanoparticles, NP.

Sample	T_{onset} (°C)	T_{max} (°C)	T_{final} (°C)	Weight loss (%)	Residue (%)
KL	136/313	149/347	171/450	5/48.5	46.5
AcKL-130	137/313	176/361	194/410	7/50	43
AcKL-140	135/315	186/373	198/410	6.5/57.5	36
AcKL-150	112/315	177/375	211/420	6/63	31
AcKL-160	129/287	157/377	192/416	2/56	42
FAcKL	193	377	426	66	34
NP	178/331	249/369	268/418	12/51.5	36.5

Note: Each respective thermal event is indicated by using a forward slash.

presents a 5 % weight loss in this region, whereas lignin nanoparticles (NP) exhibited a remarkable increase (12 %). The observations are likely related to a decrease in the number of interunit linkages, increasing the ratio of functional groups [48].

The balance between (hydroxyl group) dehydration and deacetylation in acetylated lignins may take place during the first degradation step. Therefore, for low-T microwave-assisted acetylation (AcKL-130-150), the weight loss during the first degradation step remained virtually unaffected. However, at high-T microwave-assisted acetylation (160 °C), the lower hydroxyl group content together with the slight increase of acetyl groups reduced the weight loss (2 %). By contrast, the thermogram of the reference acetylated lignin (FAcKL) did not show any detectable mass loss in hydroxyl group dehydration/deacetylation temperature range, supporting a low content of -OH groups, as observed in NMR. Hence, an enhanced stability of the acetyl groups is introduced, which may overlap with the rupture of the main inter-unit bonds.

Important differences were found considering the rupture of the main inter-unit linkages, which generate the most extensive losses. In general, the highest weight losses associated with the above thermal event occurred at the highest temperatures used during microwave-assisted acetylation, leading to a lower residual mass (from 46.5 % down to 31 %). Both chemical and mechanical modifications (acetylation and reduced particle size) have a similar effect as far as lowering the residual mass, given the alterations to the structure that facilitate degradation [40,49].

FTIR analysis (Fig. S2, supporting information) shows that the hydroxyl groups stretching vibration band of the unmodified sample, centered at around 3360 cm^{-1}, shifted to 3520 cm^{-1} upon acetylation. A shift to a higher wavenumber implies a lower degree of structuration [50], indicating that the presence of acetyl moieties prevents hydrogen bonding [51]. Unlike acetylated samples, the unmodified sample, KL and especially NP, exhibit a wide absorption peak in the range 3100–3600 cm^{-1}, as expected by the higher concentration of hydroxyl groups. By contrast, a much sharper and narrower absorption band was observed for the acetylated samples, with decreasing intensity as the acetylation temperature increased. Therefore, FTIR data suggest a gradual decrease in the hydroxyl group content, in agreement with NMR results. A noteworthy increase in the intensity of the C═O bonds stretching band, centered at 1760 and 1747 cm^{-1}, occurred in the acetylated samples, as a result of the acetylation reaction.

The water contact angle increased with acetylation (Table 3). The highest value, 69°, was obtained for FAcKL. The ANOVA analysis (at a 5 % significance level) indicated significant differences between KL and acetylated lignins, as well as between AcKL-130 and AcKL-140. However, when AcKL-150, AcKL-160 and FAcKL are compared, no major differences are noted. This may be a consequence of the high acetylation degree of these samples.

Apart from the structural changes, visible differences between the unmodified and the modified lignins are observed by SEM (Fig. 3). First, KL showed clusters, typically spherical, with diameters >40 μm. Instead, the samples produced by microwave-assisted acetylation (AcKL-130, 140, 150 and 160) exhibit important morphological changes: non-spherical shapes, and highly porous structures [52]. FAcKL and AcKL images highlight the significance of processing, aggregation and differences in particle size (Fig. S3, supporting information). The lignin nanoparticles (NP, Fig. 3) showed uneven size distribution, with diameters of up to 30 nm, similar to sizes reported earlier [39]. More detailed SEM images under different magnifications for KL, NP and AcKL-130 are included in Fig. S4 (supporting information).

3.2. Dispersion of NP in oil

Both KL and NP were tested in diverse oil media, i.e., sunflower, olive and castor oil, to assess the stabilization and rheological characteristics of the systems. Regardless of the oil used, a significant phase separation, after a few minutes, was clearly observed in dispersions of KL at 10–30

Table 3
WCA of KL and the acetylated lignins studied.

Sample	Contact angle
KL	54 ± 2
AcKL-130	62 ± 2
AcKL-140	65 ± 2
AcKL-150	67 ± 2
AcKL-160	66 ± 1
FAcKL	69 ± 3

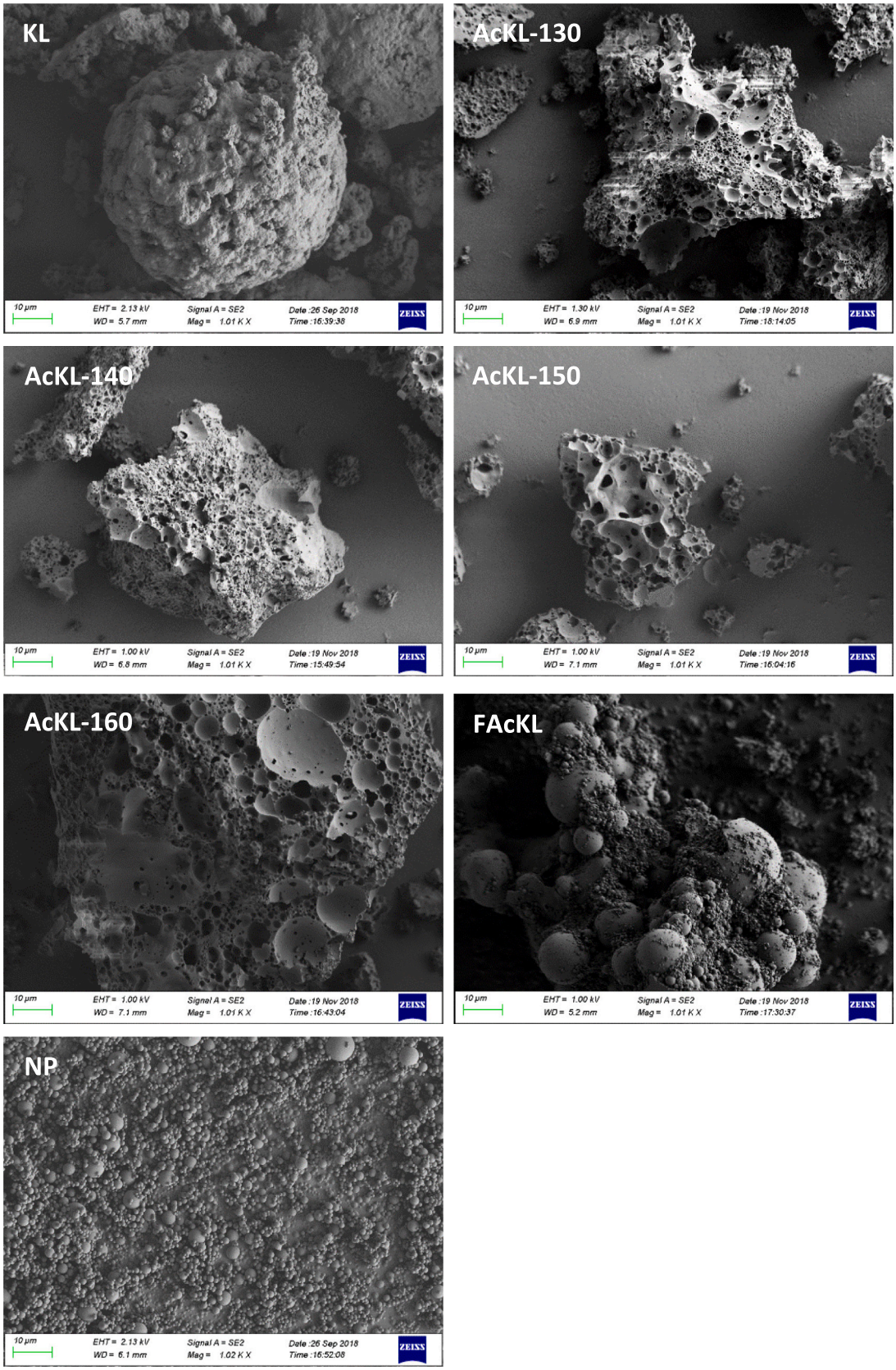

Fig. 3. SEM images of KL, AcKL, FAcKL, and NP samples.

wt% concentration. Nonetheless, when lignin nanoparticles were considered, phase separation was substantially reduced, suggesting that particle size plays a stabilizing role (note that NP/CO blends showed good stability after several days). The CO mixed with NP (10 wt%) showed phase separation (11 % v/v) after four days, whereas the 40 wt% NP dispersion was stable for several months (see Fig. S5 for KL/CO and NP/CO systems).

The increased concentration led not only to a higher stabilization but also to a reinforcement of the rheological properties: at high NP concentration, the shear-thinning behavior was enhanced (more pronounced reduction of viscosity at low and medium shear rates), which clearly indicated a higher degree of structuration (Fig. 4a) [20,53]. The shear thinning character was accompanied by a tendency to reach a viscosity plateau at high shear rates. Consequently, the viscous flow response of the blends fitted Sisko's model [54], which takes into account both shear-thinning behavior and limiting Newtonian viscosity at a high shear rate:

$$\eta = \eta_\infty + k\dot{\gamma}^{n-1} \quad (2)$$

where η_∞ depicts the high-shear rate limiting viscosity and k and n correspond to the consistency and flow indexes, respectively. The values of k and η_∞ increased with NP concentration while n decreases, reflecting a more pronounced shear-thinning response (Table 4).

G" (loss modulus) > G' (storage modulus) at 10 and 20 wt% concentration, reflecting a liquid-like behavior. However, G' > G" (low-frequency range) at 30 wt% NP concentration, indicating a higher structuration, close to the critical gel response [55]. Finally, a gel-like response was obtained when the NP concentration was raised to 40 wt % (Fig. 4b).

The ability of NP to thicken CO, in contrast to KL, is likely a consequence of the particle size (much lower for NP) and associated higher surface area (enhanced functional group accessibility) which promote interparticle interactions and hydrogen bonding with CO triglyceride. Note that the long-term stabilization was only achieved at NP concentrations between 30 and 40 wt%.

Table 4
Sisko fitting parameters (Eq. (2)) for gel-like dispersions of lignin in castor oil (NP + CO, OAcKL and OFAcKL) and given W/O emulsions (E8% FAcKL CO/W 9/1 and E8% FAcKL CO/W 7/3). CO: castor oil, NP: lignin nanoparticles, OAcKL: oleogels with acetylated lignin by microwave method at different temperatures, OFAcKL: oleogel with acetylated lignin by the solvent method, E8% FAcKL CO/W 9/1: emulsion prepared with a 8 wt% FAcKL and CO and water in 9/1 ratio, E10% FAcKL CO/W 7/3: emulsion prepared with a 10 wt% FAcKL and CO and water in a 7/3 ratio.

Sample	n	k (mPa·s^n)	η_∞ (mPa·s)
NP + CO (10 %)	0.58	210	556
NP + CO (20 %)	0.52	342	665
NP + CO (30 %)	0.42	992	1430
NP + CO (40 %)	0.23	1497	1750
OAcKL-130	0.33	10,585	28,581
OAcKL-140	0.34	3457	9355
OAcKL-150	0.16	2226	103
OAcKL-160	0.01	4275	1265
OFAcKL	0.18	1327	3737
E8% FAcKL CO/W 9/1	0.31	3598	1135
E10% FAcKL CO/W 7/3	0.43	10,097	–

3.3. Acetylated lignin dispersions in CO

The acetylated lignins were dispersed in CO at several concentrations but only those at 30 wt% ML content evidenced long-term stability, further improving the already discussed performance of NP. The viscous flow and viscoelastic response of the 30 wt% ML/CO blends are shown in Fig. 4c and d respectively, which resulted in gel-like systems. Conventionally acetylated lignin (FAcKL) yields a dispersion with values of the SAOS functions higher than those found with NP at the same concentration and, at the same time, exhibits a higher gel strength as the differences between G' and G" values indicate, i.e. higher relative elasticity. A pseudo-plateau region as those for crosslinked lignin and castor oil-based systems [2,15,18] was also exhibited. Regarding the viscous flow curves, higher viscosity values than those found for the NP dispersion at the same concentration were obtained, and similar to those achieved with NP at 40 wt% (see for instance k and n values, Table 4). The superior effect of lignin acetylation to improve the mechanical

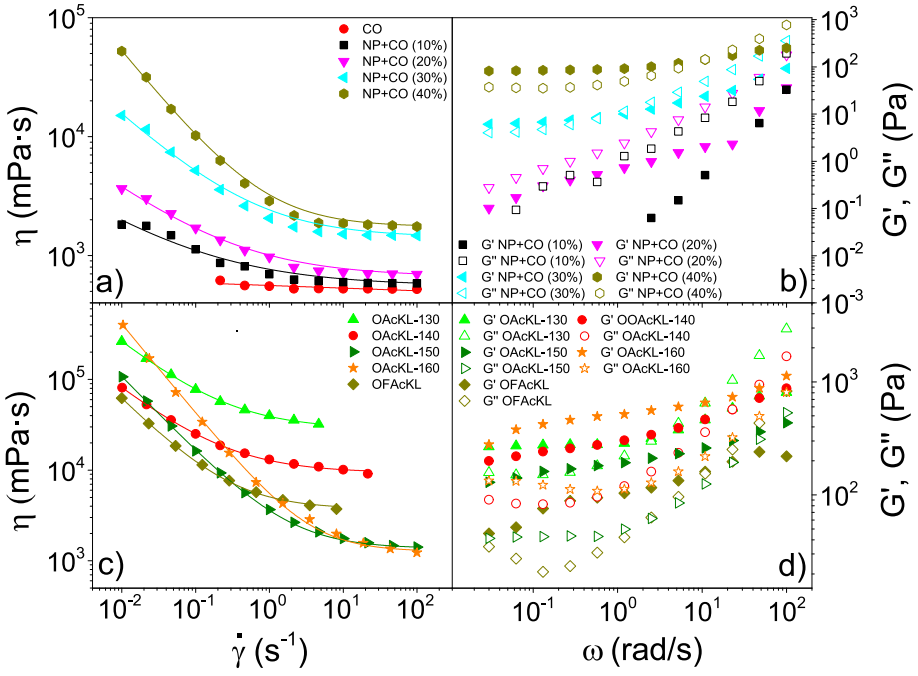

Fig. 4. Viscous flow response (left) and linear viscoelastic behavior (right) for different gel-like dispersions of lignin in castor oil (CO): CO and NP + CO blends, a) and b). Acetylated lignin in CO (OAcKL and OFAcKL), c) and d). NP: lignin nanoparticles.

properties of the gel-like dispersions, relative to the effect of reduced particle size, shows similar tendencies to those observed in lignin-based thermoplastic polymers [56].

The microwave-assisted acetylation allowed control of the acetylation and made possible the synthesis of acetylated lignins with a lower degree of substitution compared to the reference method. The less acetylated lignin (lowest microwave temperature, AcKL-130) generated a physically stable dispersion with soft gel-like characteristics. This system showed a G' / G" crossover at intermediate frequencies, similar to the behavior found for the 30 wt% NP dispersion (Fig. 4d). Remarkably, the acetylated KL (AcKL-130) showed viscoelastic moduli almost one order of magnitude higher compared to FAcKL. An increase in processing temperature, from 130 to 140 °C, resulting in a DS increase from 76 to 82 %, did not produce significant changes in G' but lowered G", increasing gel strength. In addition, a well-developed plateau region in the mechanical spectra was observed in most of the frequency range, with a crossover at high frequencies. A more severe microwave treatment (150 °C) improved the gel-like characteristics, lowering the SAOS

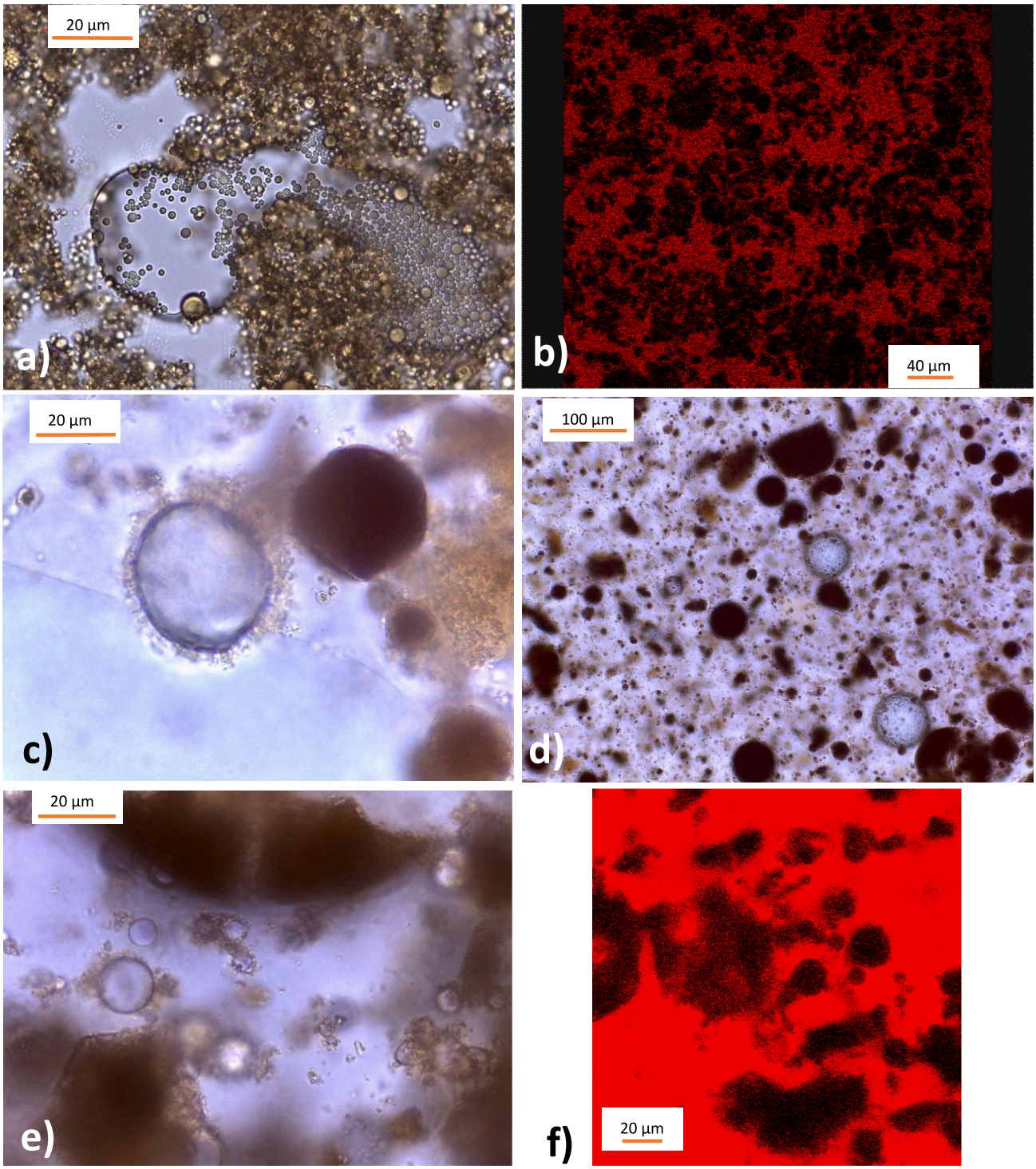

Fig. 5. Optical (a, c, d and e) and confocal microscopy images (b and f) of water-in-oil emulsions stabilized with NP (a and b), FAcKL (c and d) and AcKL-140 (e and f). Water/CO ratio: 10/90.

moduli. Therefore, a higher DS produced a lower viscoelastic response and an enhanced gel-like response with the increased degree of acetylation. The results can be rationalized by the hydrophobic interactions between the castor oil and the modified lignin. Similar findings apply to acylated chitosan, which forms gel-like dispersions in castor oil [25,57]. The viscosity profiles corroborate the above-discussed. Thus, higher viscosity values were obtained for less acetylated lignin dispersions (Fig. 4c), however, more pronounced shear thinning character, i.e., lower flow indices, were observed for highly acetylated lignin dispersions. The results indicate more structured and shear-sensitive systems (Fig. 4c, Table 4).

A particular behavior was displayed by the lignin acetylated at the highest temperature (AcKL-160). In this case, a relatively strong gel-like system, with an extended plateau region and high values of both viscoelastic moduli were obtained (Fig. 4d). In addition, a very high viscosity at low shear rates and extremely sharp shear thinning behavior were noted (Fig. 4c). This anomalous behavior observed with the dispersion of AcKL-160 is likely a result of the smaller aggregated particle size or structural units, (Fig. S6 and S7, supporting information). Other effects induced by the acetylation conditions, such as polymerization (related to an increased loss in hydroxyl groups relative to DS) are possible [58], which could explain the slight increase of acetyl groups and decrease in hydroxyl groups (Table 1).

3.4. Lignin-stabilized water-in-oil emulsions

The ability of modified lignin to thicken CO has been leveraged to trap water within the oil and generate Pickering emulsions (stable for at least several weeks) [59]. The systems prepared with a low ML content (1–5 wt%) did not generate stable Pickering emulsions. Stable Pickering emulsions were obtained at an acetylated lignin concentration of 8 wt% (% based on total mass). The emulsions were produced using a water/CO ratio of 10/90 where either NP or acetylated lignins were previously dispersed in the oil phase. As can be observed in Fig. 5, both optical and confocal images demonstrated the successful formation of water-in-oil Pickering emulsions stabilized by NP, FAcKL and AcKL-140 samples (see additional images in supporting information Fig. S8, S9 and S10). The water droplets within the oil matrix were generally surrounded by lignin nanoparticles, NP, thus stabilizing the W/O interface. Some particles were shown to be inside the water droplets, as a consequence of the high hydrophilic character provided by the high hydroxyl group content [48]. The droplets in NP-based emulsion were not spherical and showed a heterogeneous size distribution, a consequence of the low-energy process used to prepare the emulsions. FAcKL-based W/O emulsions presented more uniform water droplet distribution. Acetylated lignins were not observed inside the water droplets, given their enhanced hydrophobic character relative to KL (FAcKL particles appear only surrounding the water droplets, Fig. 5c). AcKL140-based W/O emulsion was prepared by applying higher shear/energy (using a rotor-stator homogenizer), leading to much smaller water droplets (Fig. S10). Finally, the highest water content in stable W/O emulsions prepared with FAcKL corresponded to 30 wt%, Fig. S11.

Both viscous flow and linear viscoelastic properties of selected emulsions are shown in Fig. 6a and b, respectively. The storage modulus relative to ML-CO system was increased, by two orders of magnitude, by the addition of 10 wt% water, i.e. in the emulsified form. Such improvement was further enhanced at 30 wt% water concentration. Similar observations apply to viscosity, in agreement with previous studies performed with W/O emulsions [60,61]. However, the flow index was higher for the 10 wt% water emulsion (Table 4), whilst the tendency to reach a high-shear rate-limiting viscosity, η_∞, was not observed in the case of the 30 wt% water emulsion.

4. Conclusions

We show acetylated lignin for its ability to thicken castor oil and the effect of lignin acetylation and particle size. First, dispersions of unmodified lignin nanoparticles dispersed in castor oil displayed long-term stability and gel-like properties at 40 wt% concentration. In this latter condition, a consistency index and storage modulus higher than 1.5 Pa·s and 10^2 Pa were noted, respectively. The acetylated lignin further improved the viscoelasticity of gel-like dispersions. An increase of storage and loss moduli of more than one decade for reference acetylated lignin compared to results obtained with unmodified lignin nanoparticles at the same concentration was evinced. The microwave-assisted-acetylated lignins provided even higher viscoelasticity, depending on the reaction temperature or the compatibility between lignin particles and castor oil. A higher lignin acetylation degree generally yielded lower viscosity values and a more pronounced shear-thinning character of the gel-like dispersions, as well as higher relative elasticity. The thickening ability of lignin in castor oil was exploited to formulate water-in-oil Pickering emulsions. Both lignin nanoparticles

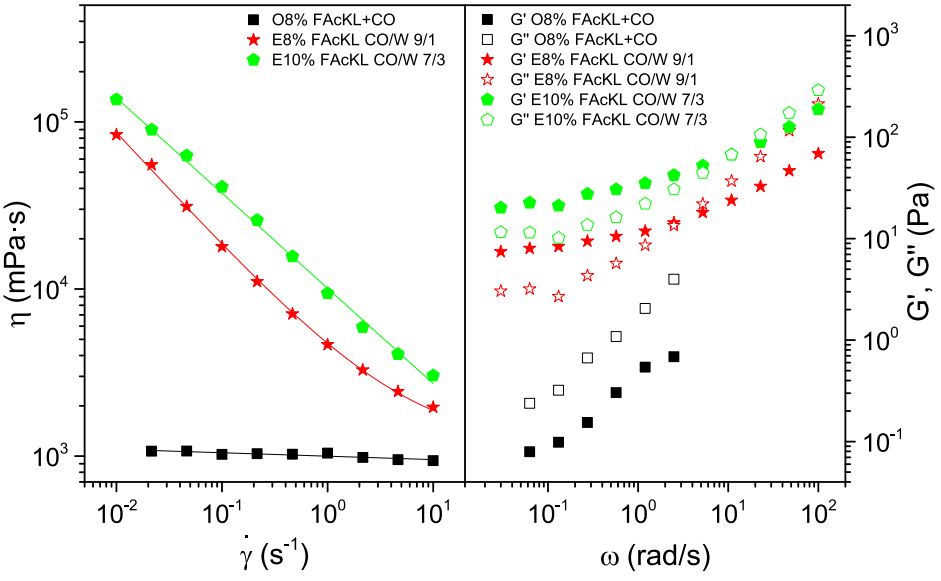

Fig. 6. left) Viscous flow curves and right) linear viscoelastic functions spectra of FAcKL-stabilized water-in-oil Pickering emulsions with 9/1 and 7/3 oil/water mass ratios compared to the gel-like dispersion with 8 wt% FAcKL.

and acetylated lignins stabilized emulsions at a water-to-oil ratio of 10/90 (8–10 wt% modified lignin concentration). The lignin with the highest acetylation degree was effective in stabilizing emulsions at a higher volume of the internal phase (30/70 water/oil emulsions).

CRediT authorship contribution statement

Antonio M. Borrero-López: Conceptualization, Software, Validation, Formal analysis, Investigation, Writing – original draft, Visualization, Project administration, Funding acquisition. **Ling Wang:** Methodology, Investigation, Resources, Writing – review & editing, Supervision. **Haiming Li:** Conceptualization, Resources. **Tainise V. Lourençon:** Software, Formal analysis, Resources, Writing – review & editing. **Concepción Valencia:** Conceptualization, Methodology, Project administration, Funding acquisition, Investigation, Writing – review & editing. **José M. Franco:** Conceptualization, Methodology, Project administration, Funding acquisition, Investigation, Writing – review & editing. **Orlando J. Rojas:** Methodology, Supervision, Investigation, Writing – review & editing.

Declaration of competing interest

The authors declare that they have no known competing financial interests or personal relationships that could have appeared to influence the work reported in this paper.

Acknowledgments

This work is part of the research project (PID2021-125637OB-I00) funded by MCIN/AEI/10.13039/501100011033 and by "ERDF A way of making Europe" (EU) and the project Grasas lubricantes basadas en materiales lignocelulósicos y aceites residuales y/o vegetales (ReGrease), funded by Cátedra Fundación CEPSA. A.M.B-L. received a PhD Research Grant from the Ministerio de Educación, Cultura y Deporte (FPU16/03697). The collaboration with the University of Aalto has been possible thanks to the grants EST17/00875 and EST18/00577 from the Ministerio de Educación y Formación Profesional. Funding for open access charge: Universidad de Huelva / CBUA. The financial support is gratefully acknowledged.

Appendix A. Supplementary data

Supplementary data to this article can be found online at https://doi.org/10.1016/j.ijbiomac.2023.124941.

References

[1] A.R. Patel, N. Cludts, M.D. Bin Sintang, B. Lewille, A. Lesaffer, K. Dewettinck, Polysaccharide-based oleogels prepared with an emulsion-templated approach, ChemPhysChem. 15 (2014) 3435–3439, https://doi.org/10.1002/cphc.201402473.
[2] A.M. Borrero-López, A. Blánquez, C. Valencia, M. Hernández, M.E. Arias, M. E. Eugenio, Ú. Fillat, J.M. Franco, Valorization of soda lignin from wheat straw solid-state fermentation: production of Oleogels, ACS Sustain. Chem. Eng. 6 (2018) 5198–5205, https://doi.org/10.1021/acssuschemeng.7b04846.
[3] A.R. Patel, Alternative routes to oil structuring, springer, N. Y. (2015), https://doi.org/10.1007/978-3-319-19138-6.
[4] C.M. Phillips, E. Kesse-Guyot, R. McManus, S. Hercberg, D. Lairon, R. Planells, H. M. Roche, High dietary saturated fat intake accentuates obesity risk associated with the fat mass and obesity–associated gene in adults, J. Nutr. 142 (2012) 824–831, https://doi.org/10.3945/jn.111.153460.
[5] N.L.G. Institute, NLGI: Lubricating Greases Guide, 5th Edition, Kansas City, 2006.
[6] T. Shen, D. Wang, J. Yun, Q. Liu, X. Liu, Z. Peng, Mechanical stability and rheology of lithium-calcium-based grease containing ZDDP, RSC Adv. 6 (2016) 11637–11647, https://doi.org/10.1039/c5ra20288d.
[7] X. He, M. Iasmin, L.O. Dean, S.E. Lappi, J.J. Ducoste, F.L. De Los Reyes, Evidence for fat, oil, and grease (FOG) deposit formation mechanisms in sewer lines, Environ. Sci. Technol. 45 (2011) 4385–4391, https://doi.org/10.1021/es2001997.
[8] W.J. Bartz, Lubricants and the environment, Tribol. Int. 31 (1998) 35–47, https://doi.org/10.1016/S0301-679X(98)00006-1.
[9] A.M. Borrero-López, C. Valencia, J.M. Franco, Lignocellulosic materials for the production of biofuels , biochemicals and biomaterials and applications of lignocellulose-based polyurethanes: a review, Polymers (Basel). 14 (2022) 881, https://doi.org/10.3390/polym14050881.
[10] R. Gallego, J.F. Arteaga, C. Valencia, M.J. Díaz, J.M. Franco, Gel-like dispersions of HMDI-cross-linked lignocellulosic materials in Castor oil: toward completely renewable lubricating grease formulations, ACS Sustain. Chem. Eng. 3 (2015) 2130–2141, https://doi.org/10.1021/acssuschemeng.5b00389.
[11] E. Cortés-Triviño, C. Valencia, M.A. Delgado, J.M. Franco, Rheology of epoxidized cellulose pulp gel-like dispersions in castor oil: influence of epoxidation degree and the epoxide chemical structure, Carbohydr. Polym. 199 (2018) 563–571, https://doi.org/10.1016/j.carbpol.2018.07.058.
[12] A.M. Borrero-López, C. Valencia, A. Blánquez, M. Hernández, M.E. Eugenio, J. M. Franco, Cellulose pulp- and castor oil-based polyurethanes for lubricating applications: influence of streptomyces action on barley and wheat straws, Polymers (Basel). 12 (2020) 2822, https://doi.org/10.3390/polym12122822.
[13] R. Gallego, J.F. Arteaga, C. Valencia, J.M. Franco, Isocyanate-functionalized chitin and chitosan as gelling agents of castor oil, Molecules. 18 (2013) 6532–6549, https://doi.org/10.3390/molecules18066532.
[14] R. Sánchez, C. Valencia, J.M. Franco, Rheological and Tribological characterization of a new Acylated chitosan-based biodegradable lubricating grease: a comparative study with traditional Lithium and calcium greases, Tribol. Trans. 57 (2014) 445–454, https://doi.org/10.1080/10402004.2014.880541.
[15] E. Cortés-Triviño, C. Valencia, J.M. Franco, Influence of epoxidation conditions on the rheological properties of gel-like dispersions of epoxidized Kraft lignin in castor oil, Holzforschung. 71 (2017) 777–784, https://doi.org/10.1515/hf-2017-0012.
[16] A.M. Borrero-López, F.J. Santiago-Medina, C. Valencia, M.E. Eugenio, J.M. Franco, Valorization of Kraft lignin as thickener in Castor oil for lubricant applications, J. Renew. Mater. 6 (2018) 347–361, https://doi.org/10.7569/JRM.2017.634160.
[17] J.F. Rubio-Valle, M.C. Sánchez, C. Valencia, J.E. Martín-Alfonso, J.M. Franco, Electrohydrodynamic processing of pvp-doped Kraft lignin micro- and nano-structures and application of electrospun nanofiber templates to produce oleogels, Polymers (Basel). 13 (2021), https://doi.org/10.3390/polym13132206.
[18] A.M. Borrero-López, C. Valencia, D. Ibarra, I. Ballesteros, J.M. Franco, Lignin-enriched residues from bioethanol production: chemical characterization, isocyanate functionalization and oil structuring properties, Int. J. Biol. Macromol. 195 (2022) 412–423, https://doi.org/10.1016/j.ijbiomac.2021.11.185.
[19] R. Gallego, J.F. Arteaga, C. Valencia, J.M. Franco, Rheology and thermal degradation of isocyanate-functionalized methyl cellulose-based oleogels, Carbohydr. Polym. 98 (2013) 152–160, https://doi.org/10.1016/j.carbpol.2013.04.104.
[20] A.M. Borrero-López, C. Valencia, J.M. Franco, Rheology of lignin-based chemical oleogels prepared using diisocyanate crosslinkers: effect of the diisocyanate and curing kinetics, Eur. Polym. J. 89 (2017) 311–323, https://doi.org/10.1016/j.eurpolymj.2017.02.020.
[21] A.M. Borrero-López, A. Blánquez, C. Valencia, M. Hernández, M.E. Arias, J. M. Franco, Influence of solid-state fermentation with Streptomyces on the ability of wheat and barley straws to thicken castor oil for lubricating purposes, Ind. Crop. Prod. 140 (2019), 111625, https://doi.org/10.1016/j.indcrop.2019.111625.
[22] G. Domínguez, A. Blánquez, A.M. Borrero-López, C. Valencia, M.E. Eugenio, M. E. Arias, J. Rodríguez, M. Hernández, Eco-friendly Oleogels from functionalized Kraft lignin with laccase SilA from Streptomyces ipomoeae : an opportunity to replace commercial lubricants, ACS Sustain. Chem. Eng. 9 (2021) 4611–4616, https://doi.org/10.1021/acssuschemeng.1c00113.
[23] M. Borrego, J.E. Martín-Alfonso, C. Valencia, M.C. del Sánchez, J.M. Franco, Developing electrospun ethylcellulose nanofibrous webs: an alternative approach for structuring castor oil, ACS Appl. Mater. Interfaces 4 (2022) 7217–7227, https://doi.org/10.1021/acsapm.2c01090.
[24] J.F. Rubio-Valle, M.C. Sánchez, C. Valencia, J.M. Franco Martín-Alfonso, Production of lignin / cellulose acetate fiber-bead structures by electrospinning and exploration of their potential as green structuring agents for vegetable lubricating oils, Ind. Crop. Prod. 188 (2022), 115579, https://doi.org/10.1016/j.indcrop.2022.115579.
[25] R. Sánchez, G.B. Stringari, J.M. Franco, C. Valencia, C. Gallegos, Use of chitin, chitosan and acylated derivatives as thickener agents of vegetable oils for bio-lubricant applications, Carbohydr. Polym. 85 (2011) 705–714, https://doi.org/10.1016/j.carbpol.2011.03.049.
[26] A. Shrotri, H. Kobayashi, A. Fukuoka, Catalytic conversion of structural carbohydrates and lignin to chemicals, in: C. Song (Ed.), Advances in Catalysis, Elsevier Inc., Amsterdam, 2017, pp. 59–123, https://doi.org/10.1016/bs.acat.2017.09.002.
[27] F.S. Chakar, A.J. Ragauskas, Review of current and future softwood Kraft lignin process chemistry, Ind. Crop. Prod. 20 (2004) 131–141, https://doi.org/10.1016/j.indcrop.2004.04.016.
[28] N.D. Patil, N.R. Tanguy, N. Yan, Lignin interunit linkages and model compounds, in: O. Faruk, M. Sain (Eds.), Lignin in Polymer Composites, Elsevier Inc., Amsterdam, 2015, pp. 27–47, https://doi.org/10.1016/B978-0-323-35565-0.00003-5.
[29] M.R.V. Bertolo, L.B. Brenelli de Paiva, V.M. Nascimento, C.A. Gandin, M.O. Neto, C.E. Driemeier, S.C. Rabelo, Lignins from sugarcane bagasse: renewable source of nanoparticles as Pickering emulsions stabilizers for bioactive compounds encapsulation, Ind. Crop. Prod. 140 (2019), 111591, https://doi.org/10.1016/j.indcrop.2019.111591.
[30] L. Dai, Y. Li, F. Kong, K. Liu, C. Si, Y. Ni, Lignin-based nanoparticles stabilized Pickering emulsion for stability improvement and thermal-controlled release of trans -resveratrol, ACS Sustain. Chem. Eng. 7 (2019) 13497–13504, https://doi.org/10.1021/acssuschemeng.9b02966.

[31] G. Shulga, S. Livcha, B. Neiberte, A. Verovkins, S. Vitolina, E. Zhilinska, The effect of pH on the ability of different lignins to stabilize the oil-in-water emulsion, IOP Conf. Ser. Mater. Sci. Eng. (2019), https://doi.org/10.1088/1757-899X/500/1/012011, p. 012011.
[32] K. Chen, Y. Qian, S. Wu, X. Qiu, D. Yang, L. Lei, Neutral fabrication of UV-blocking and antioxidation lignin-stabilized high internal phase emulsion encapsulates for high efficient antibacterium of natural curcumin, Food Funct. 10 (2019) 3543–3555, https://doi.org/10.1039/c9fo00320g.
[33] Z. Zhang, Y. Zhang, Z. Lin, A. Mulyadi, W. Mu, Y. Deng, Butyric anhydride modified lignin and its oil-water interfacial properties, Chem. Eng. Sci. 165 (2017) 55–64, https://doi.org/10.1016/j.ces.2017.02.025.
[34] J. Gould, G. Garcia-Garcia, B. Wolf, Pickering particles prepared from food waste, Materials (Basel). 9 (2016) 791, https://doi.org/10.3390/ma9090791.
[35] G. Colucci, A. Santamaria-echart, S.C. Silva, I.P.M. Fernandes, C.C. Sipoli, M. F. Barreiro, Development of water-in-oil emulsions as delivery vehicles and testing with a natural antimicrobial extract, Molecules. 25 (2020) 2105, https://doi.org/10.3390/molecules25092105.
[36] Q. Zhu, Y. Pan, X. Jia, J. Li, M. Zhang, L. Yin, Review on the stability mechanism and application of water-in-oil emulsions encapsulating various additives, Compr. Rev. Food Sci. Food Saf. 18 (2019) 1660–1675, https://doi.org/10.1111/1541-4337.12482.
[37] B.L. Tardy, J.J. Richardson, J. Guo, J. Lehtonen, M. Ago, O.J. Rojas, Lignin nano- and microparticles as template for nanostructured materials: formation of hollow metal-phenolic capsules, Green Chem. 20 (2018) 1335–1344, https://doi.org/10.1039/c8gc00064f.
[38] A. Penkina, O. Antikainen, M. Hakola, S. Vuorinen, T. Repo, J. Yliruusi, P. Veski, K. Kogermann, J. Heinämäki, Direct compression of cellulose and lignin isolated by a new catalytic treatment, AAPS PharmSciTech 14 (2013) 1129–1136, https://doi.org/10.1208/s12249-013-0002-x.
[39] M. Ago, S. Huan, M. Borghei, J. Raula, E.I. Kauppinen, O.J. Rojas, High-throughput synthesis of lignin particles (~30 nm to ~2 μm) via aerosol flow reactor: size fractionation and utilization in Pickering emulsions, ACS Appl. Mater. Interfaces 8 (2016) 23302–23310, https://doi.org/10.1021/acsami.6b07900.
[40] P. Buono, A. Duval, P. Verge, L. Averous, Y. Habibi, New insights on the chemical modification of lignin: acetylation versus Silylation, ACS Sustain. Chem. Eng. 4 (2016) 5212–5222, https://doi.org/10.1021/acssuschemeng.6b00903.
[41] N.G. Kostyukevich, D.V. Evtyugin, A.B. Nikandrov, Molecular-weight characteristics of oxygen-organosolv lignins, Izv Vyss. Uchebn Zaved Lesn Zh. 2 (3) (1993) 131–137.
[42] A. Granata, D.S. Argyropoulos, 2-Chloro-4,4,5,5-tetramethyl-1,3,2-dioxaphospholane, a reagent for the accurate determination of the uncondensed and condensed phenolic moieties in Lignins, J. Agric. Food Chem. 43 (1995) 1538–1544, https://doi.org/10.1021/jf00054a023.
[43] M. Balakshin, E. Capanema, On the quantification of lignin hydroxyl groups with ^{31}P and ^{13}C NMR spectroscopy, J. Wood Chem. Technol. 35 (2015) 220–237, https://doi.org/10.1080/02773813.2014.928328.
[44] C. Liu, H. Wang, A.M. Karim, J. Sun, Y. Wang, Catalytic fast pyrolysis of lignocellulosic biomass, Chem. Soc. Rev. 43 (2014) 7594–7623, https://doi.org/10.1039/C3CS60414D.
[45] B. Prieur, M. Meub, M. Wittemann, R. Klein, S. Bellayer, G. Fontaine, S. Bourbigot, Phosphorylation of lignin: characterization and investigation of the thermal decomposition, RSC Adv. 7 (2017) 16866–16877, https://doi.org/10.1039/c7ra00295e.
[46] C. Qi, B. Li, N. Feng, X. Ma, M. Dong, X. Deng, C. Liu, Y. Wang, W. Liu, L. Luo, J. Yue, S. Liu, T. Xia, Structure and characteristics of lignin, in: J. Huang, S. Fu, L. Gan (Eds.), Lignin Chemistry and Applications, Chemical Industry Press, Beijing, 2019, pp. 25–50, https://doi.org/10.1016/b978-0-12-813941-7.00002-3.
[47] D. Ando, F. Nakatsubo, H. Yano, Thermal stability of lignin in ground pulp (GP) and the effect of lignin modification on GP's thermal stability: TGA experiments with dimeric lignin model compounds and milled wood lignins, Holzforschung. 73 (2019) 493–499, https://doi.org/10.1515/hf-2018-0137.
[48] D. Tian, J. Hu, J. Bao, R.P. Chandra, J.N. Saddler, C. Lu, Lignin valorization: lignin nanoparticles as high-value bio-additive for multifunctional nanocomposites, Biotechnol. Biofuels. 10 (2017) 192, https://doi.org/10.1186/s13068-017-0876-z.
[49] F. Monteil-Rivera, L. Paquet, Solvent-free catalyst-free microwave-assisted acylation of lignin, Ind. Crop. Prod. 65 (2015) 446–453, https://doi.org/10.1016/j.indcrop.2014.10.060.
[50] B. Podolyák, D. Kun, K. Renner, B. Pukánszky, Hydrogen bonding interactions in poly(ethylene-co-vinyl alcohol)/lignin blends, Int. J. Biol. Macromol. 107 (2018) 1203–1211, https://doi.org/10.1016/j.ijbiomac.2017.09.098.
[51] S. Kubo, J.F. Kadla, Hydrogen bonding in lignin: a fourier transform infrared model compound study, Biomacromolecules. 6 (2005) 2815–2821, https://doi.org/10.1021/bm050288q.
[52] J. Huang, M. Wang, P. Song, Y. Li, F. Xu, X. Zhang, Directed 2D nanosheet assemblies of amphiphilic lignin derivatives: formation of hollow spheres with tunable porous structure, Ind. Crop. Prod. 127 (2019) 16–25, https://doi.org/10.1016/j.indcrop.2018.10.036.
[53] X. Liu, N. Xu, W. Li, M. Zhang, W. Lou, X. Wang, Viscosity modification of lubricating oil based on high concentration silica nanoparticles colloidal system, J. Dispers. Sci. Technol. 38 (2017) 1360–1365, https://doi.org/10.1080/01932691.2016.1220319.
[54] A.W. Sisko, The flow of lubricating greases, Ind. Eng. Chem. 50 (1958) 1789–1792, https://doi.org/10.1021/ie50588a042.
[55] L. Lu, X. Liu, Z. Tong, Critical exponents for sol-gel transition in aqueous alginate solutions induced by cupric cations, Carbohydr. Polym. 65 (2006) 544–551, https://doi.org/10.1016/j.carbpol.2006.02.010.
[56] L. Dehne, C. Vila, B. Saake, K.U. Schwarz, Esterification of Kraft lignin as a method to improve structural and mechanical properties of lignin-polyethylene blends, J. Appl. Polym. Sci. 134 (2017) 44582, https://doi.org/10.1002/app.44582.
[57] R. Sánchez, G. Alonso, C. Valencia, J.M. Franco, Rheological and TGA study of acylated chitosan gel-like dispersions in castor oil: influence of acyl substituent and acylation protocol, Chem. Eng. Res. Des. 100 (2015) 170–178, https://doi.org/10.1016/j.cherd.2015.05.022.
[58] L. Hongqiang, Y. Qu, J. Xu, Microwave-assisted conversion of lignin, in: Z. Fang, R. L.J. Smith, X. Qi (Eds.), Production of Biofuels and Chemicals with Microwave, Springer, New York, 2015, pp. 61–82, https://doi.org/10.1007/978-94-017-9612-5.
[59] C. Gupta, N.R. Washburn, Polymer-grafted lignin surfactants prepared via reversible addition-fragmentation chain-transfer polymerization, Langmuir. 30 (2014) 9303–9312, https://doi.org/10.1021/la501696y.
[60] D.M.C. Neto, C.M.S. Sad, M. Silva, F.D. Santos, L.B. Pereira, R.R.B. Corona, S.R. C. Silva, J.F.P. Bassane, E.V.R. Castro, P.R. Filgueiras, W. Romão, V. Lacerda, Rheological study of the behavior of water-in-oil emulsions of heavy oils, J. Pet. Sci. Eng. 173 (2019) 1323–1331, https://doi.org/10.1016/j.petrol.2018.10.016.
[61] A.K. Yegya Raman, S. Koteeswaran, D. Venkataramani, P. Clark, S. Bhagwat, C. P. Aichele, A comparison of the rheological behavior of hydrate forming emulsions stabilized using either solid particles or a surfactant, Fuel. 179 (2016) 141–149, https://doi.org/10.1016/j.fuel.2016.03.049.